




## Optical and Raman selection rules for odd-parity clean superconductors

Shuangyuan Lu, Xu Yang , and Yuan-Ming Lu 

*Department of Physics, The Ohio State University, Columbus, Ohio 43210, USA*

 (Received 11 January 2024; revised 15 May 2024; accepted 28 May 2024; published 14 June 2024)

We derive selection rules in optical absorption and Raman scattering spectra that can determine the parity of pairing order parameters under inversion symmetry in two classes of *clean* superconductors: (1) chiral superconductors with strong spin-orbit couplings and (ii) singlet superconductors with negligible spin-orbit couplings. Experimentally, the inversion parity of pair wave functions can be determined by comparing the “optical gap”  $\Delta_{\text{op}}$  in Raman and optical spectroscopy and the “thermodynamic gap”  $2\Delta$  in specific heat measurements, and the selection rules apply when  $\Delta_{\text{op}} > 2\Delta$ . We demonstrate the selection rules for superconductivity in models of (1) doped Weyl semimetals and (2) doped graphene. Our derivation is based on the relation between pairing symmetry and the fermion projective symmetry group of a superconductor. We further derive similar selection rules for two-dimensional superconductors with twofold rotational symmetry and discuss how they apply to the superconducting state in magic-angle twisted bilayer graphene.

DOI: [10.1103/PhysRevB.109.245119](https://doi.org/10.1103/PhysRevB.109.245119)

### I. INTRODUCTION

As the best-known quantum phenomenon on the macroscopic scale, superconductivity has many important technological applications, ranging from quantum sensing [1] and quantum computing [2] to improving energy efficiency [3]. Spontaneously breaking the  $U(1)$  charge conservation symmetry in a material, superconductors (SCs) exhibit a Landau-type off-diagonal long-range order, characterized by a pairing order parameter  $\Delta(\mathbf{k})$  in momentum space (labeled by crystal momentum  $\mathbf{k}$ ), also known as the pair wave function [4–6]. Most metals and alloys are conventional superconductors, in which superconductivity is induced by the electron-phonon coupling and well described by the BCS theory, with an isotropic  $s$ -wave spin-singlet pairing order parameter. On the other hand, other types of interactions can give rise to non- $s$ -wave unconventional superconductivity [5] with many desirable properties, such as high-temperature  $d$ -wave superconductivity in cuprates with strong Coulomb repulsions [7–10] and topological superconductivity in materials with strong spin-orbit interactions [11,12]. Unique applications can arise from unconventional superconductivity, such as fault-tolerant topological qubits based on Majorana zero modes (MZMs) [13–16].

However, in the attempt to identify an unconventional superconductor, the experimental determination of the pairing symmetry has been a challenging task for almost every candidate material [4–6,17] for the following reason. To determine the symmetry of the complex pair wave function  $\Delta(\mathbf{k})$ , one needs information about both its magnitude  $|\Delta(\mathbf{k})|$  and the phase  $\arg[\Delta(\mathbf{k})]$ . Most common experimental probes are believed to be sensitive to only the magnitude of the order parameter, including penetration depth, specific heat, thermal transport, angle-resolved photoemission, and NMR spectroscopy [6,17,18]. On the other hand, phase-sensitive measurements able to probe the relative phase of the order parameter as a function of the  $\vec{k}$ -space direction require more complicated devices and measurements, such as

superconducting quantum interference device interferometry and tricrystal or tetracrystal magnetometry [6,17], which are not easily accessible for many candidate materials. Therefore, new experimental probes that can sharply determine the symmetry representation of the pairing order parameter  $\Delta(\mathbf{k})$  are highly desirable.

As one of the simplest manifestations of pairing symmetry, in the presence of inversion symmetry, the pairing order parameter can be either an even or an odd function of  $\vec{k}$ , corresponding to (conventional) even-parity and (unconventional) odd-parity superconductivity, respectively. Odd-parity superconductors are often associated with exotic physical properties, such as MZMs in the vortex core of chiral  $p$ -wave superconductors in two dimensions [19]. In this work, we derive a set of selection rules for optical absorption and Raman spectroscopy for the particle-hole continuum of Bogoliubov quasiparticle excitations in a superconductor that allows us to sharply distinguish odd-parity and even-parity superconductors. These selection rules are derived using the correspondence between the pairing symmetry and fermion projective symmetry group (PSG) in a SC, which was recently established in Ref. [20]. We demonstrate how to use the selection rules to detect the parity of pair wave functions in two systems: (1) chiral superconductors in doped Weyl semimetals, which are an example of chiral superconductors with strong spin-orbit coupling (SOC), and (2) singlet superconductors in doped graphene, which are an example of singlet superconductors with  $SU(2)$  spin rotational symmetries. For superconductors in two-dimensional (2D) materials, we establish similar selection rules for the parity of the pair wave function under a twofold rotational symmetry  $C_{2,z}$  and discuss how they apply to superconductors in magic-angle twisted bilayer graphenes (MATBGs) [21].

*Symmetry actions on Bogoliubov quasiparticles.* In the optical absorption and Raman spectroscopies of a SC, the dominating electronic contribution comes from a pair of Bogoliubov quasiparticles with opposite momenta, known as the

“particle-hole continuum” of a SC. To obtain their selection rules under a crystalline symmetry such as inversion, we need to understand how the Bogoliubov quasiparticles transform under crystalline symmetry operations. This is captured by the following Bogoliubov–de Gennes (BdG) Hamiltonian for the SC phase:

$$\hat{H}_{\text{BdG}} = \hat{H}_0 + (\hat{H}_{\text{pair}} + \text{H.c.}), \quad (1)$$

$$\hat{H}_0 = \sum_{\alpha\beta;\mathbf{k}} \hat{c}_{\mathbf{k}\alpha}^\dagger h_{\alpha\beta}(\mathbf{k}) \hat{c}_{\mathbf{k}\beta}, \quad (2)$$

$$\hat{H}_{\text{pair}} = \sum_{\alpha\beta;\mathbf{k}} \hat{c}_{\mathbf{k}\alpha}^\dagger \Delta_{\alpha\beta}(\mathbf{k}) \hat{c}_{-\mathbf{k}\beta}^\dagger, \quad (3)$$

where  $\hat{H}_0$  describes the normal state band structure  $h_{\alpha,\beta}(\mathbf{k})$  of electrons and  $\hat{H}_{\text{pair}}$  describes the Cooper pairing of electrons. We use  $\alpha$  and  $\beta$  to generally denote the spin, orbital, and sublattice indices of electrons. Under a crystalline symmetry operation  $\hat{g}$ , the electron transforms as  $\hat{g} c_{\mathbf{k}\alpha} \hat{g}^{-1} = [U_0^g(\mathbf{k})]_{\alpha\beta}^\dagger \hat{c}_{g\mathbf{k}\beta}$ , where  $U_0^g(\mathbf{k})$  is a unitary matrix. Although the normal state band structure preserves the  $\hat{g}$  symmetry as  $[\hat{g}, \hat{H}_0] = 0$ , the pairing term  $\hat{H}_{\text{pair}}$  in an unconventional SC is generally *not* invariant under crystal symmetry  $\hat{g}$  [20,22,23].

In this paper we restrict ourselves to SCs without spontaneous breaking of spin rotational symmetries; i.e., the normal state and SC belong to the same global (spin rotation) symmetry group. In this case, due to the broken  $U(1)$  charge symmetry, the pairing term  $\hat{H}_{\text{pair}}$  can acquire a phase  $e^{i\Phi_g}$  under crystal symmetry  $\hat{g}$  [20,22,23]:

$$U_0^g(\mathbf{k}) \Delta(\mathbf{k}) [U_0^g(-\mathbf{k})]^T = e^{i\Phi_g} \Delta(g\mathbf{k}). \quad (4)$$

The phase factors  $\{e^{i\Phi_g} | g \in X\}$  form a one-dimensional irreducible representation (irrep) of the crystal symmetry group  $X$ , satisfying  $e^{i(\Phi_g + \Phi_h)} = e^{i\Phi_{gh}}$  for any  $g, h \in X$ .

For the order-2 inversion symmetry  $\hat{\Gamma}$  of interest to this work, we have  $e^{i\Phi_\Gamma} = \pm 1$ , and hence,

$$U_0^\Gamma(\mathbf{k}) \Delta(\mathbf{k}) [U_0^\Gamma(-\mathbf{k})]^T = \pm \Delta(-\mathbf{k}), \quad (5)$$

where the  $+$  and  $-$  signs correspond to even and odd parity under inversion symmetry, respectively. Note that due to nontrivial transformations of the pair wave function  $\Delta(\mathbf{k})$  shown above, the BdG Hamiltonian is not invariant under the normal state symmetry  $\hat{g}$  anymore. Instead,  $\hat{H}_{\text{BdG}}$  preserves a combination  $\hat{g}'$  of normal state crystal symmetry  $\hat{g} \in X$  and a  $U(1)$  charge rotation  $e^{-i\Phi_{g'}\hat{F}/2}$ , where  $\hat{F}$  is the total fermion number:

$$\begin{aligned} \hat{g}' \hat{H}_{\text{BdG}} (\hat{g}')^{-1} &= \hat{H}_{\text{BdG}}, & \hat{g}' &= e^{-i\Phi_{g'}\hat{F}/2} \hat{g}, \\ \hat{g}' c_{\mathbf{k},\alpha} (\hat{g}')^{-1} &= e^{-i\Phi_{g'}/2} [U_0^g(\mathbf{k})]_{\alpha\beta}^\dagger \hat{c}_{g\mathbf{k},\beta}. \end{aligned} \quad (6)$$

In the case of order-2 inversion symmetry  $\Gamma$ , we have

$$(\Gamma')^2 = e^{-i\Phi_\Gamma\hat{F}} = (\pm 1)^{\hat{F}}. \quad (7)$$

In other words, inversion squares to  $\pm 1$  when acting on a fermion operator in a SC with an even or odd parity under inversion symmetry. They correspond to two different fermion PSGs [20] with distinct physical properties. In particular, we consider Bogoliubov quasiparticles (BQPs)  $\{\gamma_{\mathbf{k},a}\}$  of the BdG

Hamiltonian (1):

$$\hat{H}_{\text{BdG}} = \sum_{\mathbf{k},a} E_a(\mathbf{k}) \gamma_{\mathbf{k},a}^\dagger \gamma_{\mathbf{k},a}, \quad E_a(\mathbf{k}) \geq 0, \quad (8)$$

where  $a$  generally labels the spin or band indices of BQPs.

In optical absorption and Raman spectroscopy experiments, the dominant electronic contribution comes from a pair of BQPs with opposite momenta. Considering the inversion symmetry  $\Gamma'$  in (7) for the SC phase, we can always choose a gauge so that

$$\Gamma' \begin{pmatrix} \gamma_{\mathbf{k},a}^\dagger \\ \gamma_{-\mathbf{k},a}^\dagger \end{pmatrix} (\Gamma')^{-1} = \begin{pmatrix} \gamma_{-\mathbf{k},a}^\dagger \\ \pm \gamma_{\mathbf{k},a}^\dagger \end{pmatrix}. \quad (9)$$

This relation and Fermi statistics together lead to a gauge-invariant inversion eigenvalue for a pair of BQPs with opposite momenta:

$$\Gamma' (\gamma_{\mathbf{k},a}^\dagger \gamma_{-\mathbf{k},a}^\dagger) (\Gamma')^{-1} = \mp (\gamma_{\mathbf{k},a}^\dagger \gamma_{-\mathbf{k},a}^\dagger). \quad (10)$$

In a chiral SC with strong SOC, there is no Kramers degeneracy for BQPs at a generic momentum, and therefore, the BQP pair with the lowest energy comes from the same Bogoliubov band,  $a = 0$ . Therefore, the inversion quantum number (10) directly applies to the low-frequency spectroscopy of a chiral SC. On the other hand, in a singlet SC with  $SU(2)$  spin rotational symmetries, each Bogoliubov band has a twofold spin degeneracy  $\alpha, \beta = \uparrow, \downarrow$  at every momentum. In this case, the spin-singlet BQP pair with the lowest energy has the following gauge-invariant inversion eigenvalue:

$$\Gamma' (\epsilon^{\alpha\beta} \gamma_{\mathbf{k},0,\alpha}^\dagger \gamma_{-\mathbf{k},0,\beta}^\dagger) (\Gamma')^{-1} = \pm (\epsilon^{\alpha\beta} \gamma_{\mathbf{k},0,\alpha}^\dagger \gamma_{-\mathbf{k},0,\beta}^\dagger). \quad (11)$$

Here, band index 0 in the subscript means the lowest BdG band with a non-negative energy. Below we show how the gauge-invariant inversion eigenvalues in (10) and (11) lead to selection rules in optical absorption and Raman spectroscopy which can be used to detect the inversion parity of pairing order parameters.

## II. OPTICAL ABSORPTION SPECTROSCOPY

It was believed that optical spectroscopy via inelastic light scattering is sensitive only to the magnitude of the pairing order parameter [6,24]. Although Higgs modes have been proposed to characterize and differentiate different pairing symmetries in unconventional superconductors [25], they have proven difficult to observe in superconductors due to the nonlinear light-Higgs coupling [26]. On the other hand, the particle-hole continuum above the  $2\Delta$  threshold, created by breaking a Cooper pair and exciting two Bogoliubov quasiparticles, is the most important electronic response to inelastic optical probes in a superconductor [24]. Below we demonstrate that the aforementioned symmetry transformations on BQPs lead to distinct optical selection rules for the particle-hole continuum in SCs.

The dominant component of light-matter interaction is the coupling of the vector potential  $\mathbf{A}$  of light with the particle current operator  $\hat{\mathbf{j}}$  of the system:

$$\hat{H}_{\text{int}} = -e\mathbf{A}(t) \cdot \hat{\mathbf{j}}. \quad (12)$$

TABLE I. Selection rules for the parity of pair wave functions under inversion symmetry  $\hat{\Gamma}$  in chiral SCs with strong SOC for optical absorption spectroscopy and Raman spectroscopy.

Parity of $\Delta(\mathbf{k})$	$(\hat{\Gamma}')^2$	Parity of $\gamma_{\mathbf{k},a}^\dagger \gamma_{-\mathbf{k},a}^\dagger$	$\text{Im}\chi(2\Delta < \omega < \Delta + \Delta')$	$I_{\text{Raman}}(2\Delta < \omega < \Delta + \Delta')$
Even	+1	Odd	Nonzero	0
Odd	-1	Even	0	Nonzero

The optical absorption rate is given by the transition rate in time-dependent perturbation theory, where the first-order perturbation theory leads to

$$\begin{aligned} \sum_f w_{i \rightarrow f} &= \frac{2\pi}{\hbar} \sum_f |\langle f | \hat{H}_{\text{int}} | i \rangle|^2 \delta(E_f - E_i - \omega) \\ &= \frac{\pi e^2}{\epsilon_0 \omega} \sum_f |\langle i | \mathbf{e} \cdot \hat{\mathbf{j}} | f \rangle|^2 \delta(\omega + E_i - E_f) \quad (13) \end{aligned}$$

$$= \frac{\hbar}{\epsilon_0} \omega \text{Im}\chi(\omega) = \frac{\hbar}{\epsilon_0} \text{Re}\sigma(\omega), \quad (14)$$

where  $\mathbf{e}$  is the polarization vector of light and  $\chi(\omega) = \chi' + i\chi''$  and  $\sigma(\omega)$  are the electric susceptibility and optical conductivity in linear response theory. At zero temperature, the initial state  $|i\rangle$  is the SC ground state  $|0\rangle$ , and the final state  $|f\rangle$  is obtained by creating a zero-momentum BQP pair on the ground state so that

$$\begin{aligned} \frac{\hbar}{\epsilon_0} \omega \text{Im}\chi(T=0, \omega) &= \frac{\pi e^2}{2\epsilon_0 \omega} \sum_{\mathbf{k}, a, b} |\langle 0 | \mathbf{e} \cdot \hat{\mathbf{j}} (\gamma_{\mathbf{k},a}^\dagger \gamma_{-\mathbf{k},b}^\dagger) | 0 \rangle|^2 \\ &\quad \times \delta[\omega - E_a(\mathbf{k}) - E_b(-\mathbf{k})] + \dots, \quad (15) \end{aligned}$$

where  $\dots$  stands for other contributions from, e.g., Higgs modes or four Bogoliubov quasiparticles. If we label the bottoms of the lowest and second-lowest BQP bands as  $\Delta$  and  $\Delta'$ , respectively, with  $\Delta < \Delta'$ , for the frequency range

$$\omega < \Delta + \Delta', \quad (16)$$

only a pair of BQPs from the lowest Bogoliubov band  $a = b = 0$  contributes, which corresponds to

$$|f\rangle = \gamma_{\mathbf{k},0}^\dagger \gamma_{-\mathbf{k},0}^\dagger |0\rangle \quad (17)$$

in a chiral SC with a strong SOC or

$$|f\rangle = \epsilon^{\alpha\beta} \gamma_{\mathbf{k},0,\alpha}^\dagger \gamma_{-\mathbf{k},0,\beta}^\dagger |0\rangle \quad (18)$$

in a singlet SC with  $SU(2)$  symmetry. Since the current operator  $\hat{\mathbf{j}}$  is odd under inversion symmetry

$$\Gamma' \hat{\mathbf{j}} (\Gamma')^{-1} = -\hat{\mathbf{j}}, \quad (19)$$

Eqs. (10) and (11) immediately lead to the optical absorption selection rules summarized in Tables I and II for chiral

SCs with SOC and singlet SCs without SOC, respectively. It is worth mentioning that the above absorption selection rules recover one well-known conclusion in the single-band ( $\Delta' \rightarrow \infty$ ) limit: there is no optical absorption for  $\omega > 2\Delta$  in single-band clean  $s$ -wave SCs [27].

Below we demonstrate the absorption selection rules with two examples. First, we study superconductivity in doped magnetic Weyl semimetals [28,29] as an example of chiral SCs with strong SOC. Specifically, we consider two different pairing symmetries (see Appendix A) of zero-momentum Cooper pairs, one with even parity under inversion and another with odd parity, in the two-band model of an inversion-symmetric Weyl semimetal that breaks time reversal symmetry [28]. As shown in Fig. 1, while the electronic contribution to light absorption remains finite at all frequencies  $\omega > 2\Delta = 0$  for an even-parity SC, it vanishes at a low frequency ( $\omega < \Delta + \Delta'$  in Fig. 1) for an odd-parity SC. Here, for the even-parity SC, the energy gaps are  $\Delta = 0.5t$  and  $\Delta' = 3.5t$ . Here,  $t$  is the hopping integral defined in Appendix A, which is the characteristic energy scale of our models. The odd-parity SC state is gapless ( $\Delta = 0$ ) due to the nontrivial topological charge of the Weyl points [30]. The energy gaps are  $\Delta = 0$  and  $\Delta' = 0.5t$ . Remarkably, in the odd-parity SC, independent of the direction of light polarization  $\mathbf{e}$  (see Appendix A), there is no optical absorption even above the thermodynamic gap  $2\Delta$ , and the associated ‘‘optical gap’’ is lower bounded by  $\Delta_{\text{op}} \geq \Delta + \Delta'$ , consistent with selection rules in Table I.

Next, we study spin-singlet superconductivity in doped graphene as an example of singlet SCs with  $SU(2)$  spin rotational symmetry. Specifically, we consider two different pairing symmetries (see Appendix B) with zero center-of-mass momentum in the honeycomb lattice model of graphene with a finite chemical potential. Energy gaps for the even-parity case are  $\Delta = 0.22t$  and  $\Delta' = 0.75t$ , and those for the odd-parity case are  $\Delta = 1.1t$  and  $\Delta' = 4.2t$ . The absorption rate as a function of light frequency  $\omega$  is shown in Fig. 2. The odd-parity SC is gapless, and its absorption rate is nonzero for all frequencies. In contrast, the absorption rate of the even-parity SC is identically zero above the bulk thermodynamic gap  $2\Delta \approx 0.4t$ , until the light frequency reaches an optical gap of  $\Delta_{\text{op}} \approx 1.2t > \Delta + \Delta'$ . This demonstrates the selection rules for even-parity singlet SCs.

TABLE II. Selection rules for the parity of pair wave functions under inversion symmetry  $\hat{\Gamma}$  in singlet SCs with no SOC and hence  $SU(2)$  symmetry for optical absorption spectroscopy and Raman spectroscopy.

Parity of $\Delta(\mathbf{k})$	$(\hat{\Gamma}')^2$	Parity of $\epsilon^{\alpha\beta} \gamma_{\mathbf{k},0,\alpha}^\dagger \gamma_{-\mathbf{k},0,\beta}^\dagger$	$\text{Im}\chi(2\Delta < \omega < \Delta + \Delta')$	$I_{\text{Raman}}(2\Delta < \omega < \Delta + \Delta')$
Even	+1	Even	0	Nonzero
Odd	-1	Odd	Nonzero	0

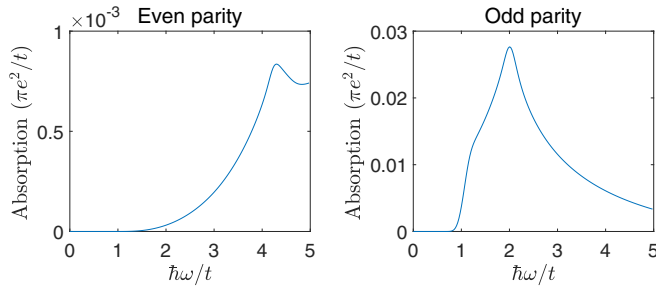


FIG. 1.  $T = 0$  absorption spectra of two chiral SCs with opposite pairing parity under inversion symmetry in a two-band model of doped Weyl semimetals [28,29] that breaks time reversal symmetry. Left:  $\Delta = 0.5t$ ,  $\Delta' = 3.5t$ . Right:  $\Delta = 0$ ,  $\Delta' = 0.5t$ .

The selection rules for optical absorption (and conductivity) in Tables I and II were previously discussed in Ref. [23] in the context of the Altland-Zirnbauer classes [31] of quadratic BdG Hamiltonians. Compared to Ref. [23], which is based on the particle-hole symmetry of the quadratic BdG Hamiltonian, the current work derives the selection rules using the relation between fermion PSGs and SC pairing symmetry [20,22], which generally applies to interacting fermions. In an interacting fermion system, since the Altland-Zirnbauer symmetry classes do not directly apply to a many-body interacting Hamiltonian, the symmetry group characterized by the fermion PSGs is required to properly describe the full symmetry of the superconducting phase. For example, in the case of global symmetries, class D corresponds to chiral superconductors without spin rotational symmetries (e.g., due to strong spin-orbit coupling), class C corresponds to chiral singlet superconductors with  $SU(2)$  spin rotational symmetries, and class CI corresponds to singlet superconductors with time reversal symmetry. As we showed above, the parity of the pairing order parameters of these three symmetry types can be detected by selection rules in the presence of inversion symmetry. Therefore, our formulation enables a generalization of the single-particle results of Ref. [23] to correlated systems with well-defined Bogoliubov quasiparticles  $\gamma_{\mathbf{k},a}$ , in a way similar to how a Fermi liquid generalizes a noninteracting Fermi gas. Moreover, compared to those in Ref. [23], our results point to a clear protocol to detect the SC pairing symmetry through a comparison of the optical gap and the

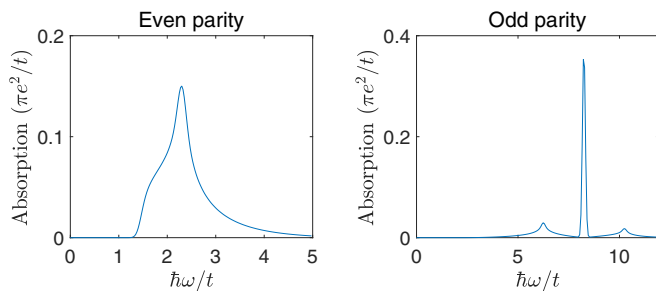


FIG. 2.  $T = 0$  absorption spectra of two singlet SCs with opposite pairing parity under inversion symmetry in the honeycomb lattice model of doped graphene. Left:  $\Delta = 0.22t$ ,  $\Delta' = 0.75t$ . Right:  $\Delta = 1.1t$ ,  $\Delta' = 4.2t$ .

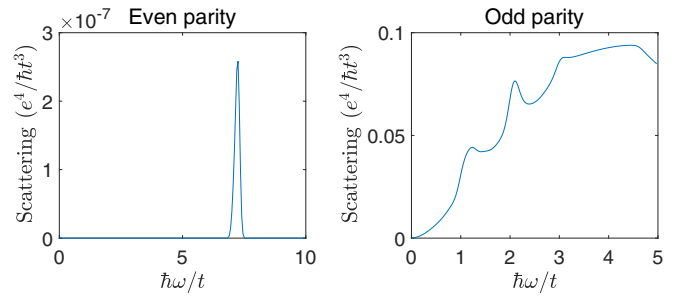


FIG. 3.  $T = 0$  Raman spectra of two chiral SCs with opposite pairing parity under inversion symmetry in a two-band model of doped Weyl semimetals. Left:  $\Delta = 0.5t$ ,  $\Delta' = 3.5t$ . Right:  $\Delta = 0$ ,  $\Delta' = 0.5t$ .

thermodynamic gap  $2\Delta$ , which can be obtained by, e.g., measuring the specific heat. Based on the above relation between fermion PSGs and the SC pairing symmetry, below we further derive different selection rules in Raman spectroscopy.

### III. RAMAN SPECTROSCOPY

The Raman differential scattering cross section is given by Fermi's golden rule [24,32,33]:

$$\frac{\partial^2 \sigma}{\partial \Omega \partial \omega_s} = \frac{e^4 \omega_s}{\hbar \omega_i} \sum_f |\langle f | e_i^\alpha e_s^\beta M^{\alpha\beta} | i \rangle|^2 \delta(\omega + E_i - E_f), \quad (20)$$

where  $e_i$  and  $e_s$  are the polarization vectors of incident and scattered light.  $\omega_i$  and  $\omega_s$  are the frequencies of the incident light and of the scattered light, respectively, and  $\omega = \omega_i - \omega_s$ .  $\hat{M}$  is the Raman scattering operator, given by

$$\begin{aligned} \langle f | e_i^\alpha e_s^\beta M^{\alpha\beta} | i \rangle &= e_i^\alpha e_s^\beta \langle f | \sum_{\mathbf{k}, \alpha, \beta} c_{\mathbf{k}, \alpha}^\dagger \frac{\partial^2 h_{\alpha, \beta}(\mathbf{k})}{\partial k^a \partial k^b} c_{\mathbf{k}, \beta} | i \rangle \\ &+ \sum_v \left[ \frac{\langle f | (\vec{j} \cdot \hat{e}_f) | v \rangle \langle v | (\vec{j} \cdot \hat{e}_i) | i \rangle}{E_v - E_i - \omega_i} \right. \\ &\left. + \frac{\langle f | (\vec{j} \cdot \hat{e}_i) | v \rangle \langle v | (\vec{j} \cdot \hat{e}_f) | i \rangle}{E_v - E_i + \omega_s} \right], \quad (21) \end{aligned}$$

where  $E_v$  labels the energy of eigenstate  $|v\rangle$ . Clearly, the  $M$  operator is even under inversion symmetry.

As a result, following the same logic as in the discussion of absorption spectroscopy, we can obtain the selection rules for Raman intensity  $I_{\text{Raman}}(\omega)$ , shown in the last columns of Tables I and II. Note that the inversion symmetry selection rules for Raman spectra are opposite those for absorption spectra. In particular, for chiral SCs with strong SOC, the Raman intensity vanishes even above the thermodynamic gap  $2\Delta$  for an even-parity pair wave function.

We also calculate Raman spectra for both our models. For the model with Weyl semimetals without  $SU(2)$ , we show results in Fig. 3. For the even-parity case, the selection rule requires the scattering to be zero below  $\Delta + \Delta'$ . For the odd-parity case, there is no selection rule, and the spectrum is not zero at any frequency because the band is gapless ( $\Delta = 0$ ).

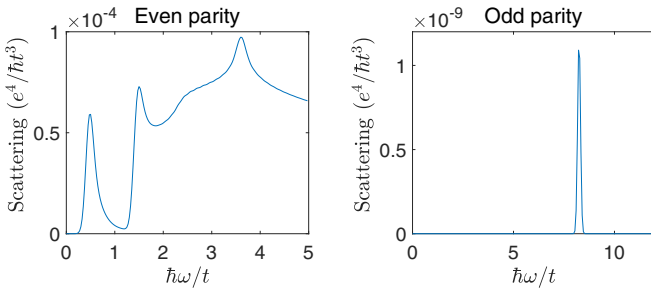


FIG. 4.  $T = 0$  Raman spectra of two singlet SCs with opposite pairing parity under inversion symmetry in the honeycomb lattice model of doped graphene. Left:  $\Delta = 0.22t$ ,  $\Delta' = 0.75t$ . Right:  $\Delta = 1.1t$ ,  $\Delta' = 4.2t$ .

The Raman spectra for SCs on a honeycomb lattice with  $SU(2)$  symmetry are shown in Fig. 4. For the even-parity case, the spectrum is not zero above energy gap  $2\Delta = 0.44t$  because there is no selection rule. For the odd-parity case, the spectrum is zero between energy gap  $2\Delta = 2.2t$  and  $\Delta + \Delta' = 5.3t$ , as required by the selection rule.

#### IV. $C_{2,z}$ SYMMETRY IN 2D SUPERCONDUCTORS

For a quasi-two-dimensional SC, the previous derivation of the selection rules for inversion symmetry  $\Gamma$  naturally generalizes to twofold rotation  $C_{2,z}$ , whose rotation axis is perpendicular to the 2D plane. There is one subtlety, however, from nontrivial  $C_{2,z}$  symmetry actions on electrons in the normal state:  $\hat{C}_{2,z}^2 = 1$  for  $SU(2)$ -symmetric 2D systems with weak SOC, or  $\hat{C}_{2,z}^2 = (-1)^{\hat{f}}$  for 2D systems with strong SOC. In a 2D singlet SC with  $SU(2)$  spin rotational symmetry, the twofold rotation  $C_{2,z}$  simply reverses both the  $x$  and  $y$  coordinates in the 2D space in the same way as the inversion symmetry. This leads to the same set of selection rules in Table II for 2D singlet SCs with  $C_{2,z}$  symmetry. On the other hand, for 2D chiral SCs with strong SOC, due to the nontrivial  $\hat{C}_{2,z}^2 = (-1)^{\hat{f}}$  action in the normal state, the  $C_{2,z}$  selection rules are opposite those of inversion symmetry, as summarized in Table III.

Below we briefly discuss one example in which such selection rules apply. By analyzing a collection of existing experimental data, Ref. [34] recently argued that the structure of SC pairing order parameters in MATBG is almost uniquely determined except for its orbital parity under  $C_{2,z}$  symmetry, which is either even ( $d$  wave) or odd ( $p$  wave). In the normal state of MATBG,  $C_{2,z}^2 = (-1)^{\hat{f}}$  arises from spontaneously generated SOC due to spin-valley locking [34], and therefore, the selection rules in Table III directly point to experimental

signatures to determine the pairing symmetry of the chiral SC in MATBG [20].

#### V. DISCUSSION AND OUTLOOK

Using the correspondence between pairing symmetry and the fermion PSG in SCs obtained recently [20,22], we derived selection rules in optical absorption and Raman scattering spectroscopy for two classes of clean SCs: (1) chiral SCs with strong SOC and (2) singlet SCs with weak SOC. In particular, the selection rules in case 1 can be applied to distinguish the inversion parity of pair wave functions in many candidate materials of chiral superconductors [35], such as  $\text{SrRuO}_4$  [36,37],  $\text{UPt}_3$  [38] and  $\text{UTe}_2$  [39]. We derive a similar set of selection rules for twofold rotational symmetry  $C_{2,z}$  in 2D SCs and discuss how they can be applied to distinguish the proposed  $d$ -wave from  $p$ -wave SCs in MATBG [34].

While this work has focused on clean SCs, it is well known that optical absorption exists above the thermodynamic gap  $2\Delta$  in dirty SCs [40–42]. Since impurities break the crystalline inversion or rotation symmetry, the selection rules derived here for clean SCs do not apply in the dirty limit, giving rise to nonzero optical and Raman responses above  $2\Delta$ . In the presence of impurities, one natural question is, How do the optical responses in absorption and Raman scattering depend on the frequency  $\omega$  above the thermodynamic gap  $2\Delta$ ? For example, even- and odd-parity SCs may have different power-law dependence on  $\omega - 2\Delta$  for optical absorption and Raman intensity. Another future direction is to generalize the current work to selection rules of optical and Raman responses in topological orders, e.g.,  $Z_2$  spin liquids, which are related to a SC by gauging the fermion parity symmetry  $Z_2^f$ . We leave these questions for future studies.

#### ACKNOWLEDGMENTS

We thank S. Ono, S. Biswas, and M. Randeria for helpful discussions and related collaborations. This work is supported by the Center for Emergent Materials at The Ohio State University, a National Science Foundation (NSF) MRSEC, through NSF Award No. DMR-2011876. Y.-M.L. acknowledges support from Grant No. NSF PHY-1748958 to the Kavli Institute for Theoretical Physics (KITP) and NSF Grant No. PHY-2210452 to the Aspen Center for Physics.

#### APPENDIX A: CHIRAL SUPERCONDUCTIVITY IN A TWO-BAND MODEL OF A DOPED WEYL SEMIMETAL

In this example, we demonstrate the phenomenon of selection rules by studying superconductivity in a doped Weyl semimetal. In this example of a doped Weyl semimetal, time reversal symmetry is broken, while inversion and  $C_4$

TABLE III. Selection rules for the parity of pair wave functions under rotational symmetry  $\hat{C}_{2,z}$  in 2D chiral SCs with strong SOC for optical absorption spectroscopy and Raman spectroscopy.

Parity of $\Delta(\mathbf{k})$	$(\hat{C}_{2,z}^2)^2$	Parity of $\gamma_{\mathbf{k},a}^\dagger \gamma_{-\mathbf{k},a}^\dagger$	$\text{Im}\chi(2\Delta < \omega < \Delta + \Delta')$	$I_{\text{Raman}}(2\Delta < \omega < \Delta + \Delta')$
Even	-1	Even	0	Nonzero
Odd	+1	Odd	Nonzero	0

TABLE IV. For each pairing term, its quantum numbers under operators  $I$  and  $C_4$  are listed. The true symmetries  $I'$  and  $C_4'$  have different symmetry fractionalization classes, and the corresponding quantum numbers  $I'^2$ ,  $C_4'^4$  and  $I'C_4'I'^{-1}C_4'^{-1}$  are listed.

$\Delta(\mathbf{k})$	$I$	$C_4$	$I'^2$	$C_4'^4$	$I'C_4'I'^{-1}C_4'^{-1}$
$\cos k_z i\sigma^y$	-1	1	-1	-1	1
$\sin k_z \sigma^x$	1	1	1	-1	1
$\sin k_z (\sigma^0 + \sigma^z)$	-1	-i	-1	1	1
$\sin k_z (\sigma^0 - \sigma^z)$	-1	i	-1	1	1
$(\cos k_x + \cos k_y) i\sigma^y$	-1	1	-1	-1	1
$(\cos k_x - \cos k_y) i\sigma^y$	-1	-1	-1	-1	1
$(\sin k_x + i \sin k_y) \sigma^x$	1	-i	1	1	1
$(\sin k_x - i \sin k_y) \sigma^x$	1	i	1	1	1
$(\sin k_x + i \sin k_y) (\sigma^0 + \sigma^z)$	-1	-1	-1	-1	1
$(\sin k_x - i \sin k_y) (\sigma^0 + \sigma^z)$	-1	1	-1	-1	1
$(\sin k_x + i \sin k_y) (\sigma^0 - \sigma^z)$	-1	1	-1	-1	1
$(\sin k_x - i \sin k_y) (\sigma^0 - \sigma^z)$	-1	-1	-1	-1	1

rotational symmetries along the  $z$  axis are preserved. To be more specific, we consider nearest-neighbor terms in a three-dimensional cubic lattice model with two orbitals on each site, and the Hamiltonian [28,29] in the momentum space is

$$h_0(\mathbf{k}) = t \sin(k_x) \sigma^x + t \sin(k_y) \sigma^y + m[2 - \cos(k_x) - \cos(k_y)] \sigma^z + t_z [\cos(k_z) - \cos(Q)] \sigma^z + \mu \sigma^0. \quad (\text{A1})$$

Here,  $t(k)$  indicates the hopping part of the Hamiltonian, and  $t$ ,  $m$ ,  $t_z$ , and  $\mu$  are real numbers. Two dimensions of matrix  $\sigma$  represent two orbitals. This Hamiltonian generally has Weyl nodes at  $\mathbf{k} = (0, 0, \pm Q)$ .

The inversion and  $C_4$  rotational symmetries act on fermions in the following way:

$$\begin{aligned} I : c_{s,\mathbf{k}} &\rightarrow \sigma_{s,s'}^z c_{s',-\mathbf{k}}, \\ C_4 : c_{s,(k_x,k_y,k_z)} &\rightarrow S_{s,s'} c_{s',(k_y,-k_x,k_z)}, \end{aligned} \quad (\text{A2})$$

where  $\sigma^z$  and  $S = \frac{1}{\sqrt{2}}(\sigma^0 + i\sigma^z)$  are the action of  $C_4$  on orbitals. The inversion and  $C_4$  rotation symmetries act on both space (momentum is changed) and spin (matrix  $\sigma$ ) degrees of freedom. In the form of a matrix, we can write

$$\begin{aligned} I : h_0(-\mathbf{k}) &\rightarrow \sigma^z h_0(\mathbf{k}) \sigma^z, \\ C_4 : h_0(-k_y, k_x, k_z) &\rightarrow S^\dagger h_0(k_x, k_y, k_z) S. \end{aligned} \quad (\text{A3})$$

To have superconductivity, we add the pairing term  $\Delta_{s_1,s_2}^\dagger(k) c_{s_1,-k} c_{s_2,k} + \text{H.c.}$  Inversion and rotational symmetries act on the pairing terms in the following way:

$$\begin{aligned} I : \Delta(-\mathbf{k}) &\rightarrow \sigma^z \Delta(\mathbf{k}) \sigma^z, \\ C_4 : \Delta(-k_y, k_x, k_z) &\rightarrow S^\dagger \Delta(k_x, k_y, k_z) S^*. \end{aligned} \quad (\text{A4})$$

Under this transformation, different pairing terms have different quantum numbers, and they are listed in Table IV.

In Table IV  $I$  and  $C_4$  are the operators defined before. We show the quantum number of each term. However, as discussed in the main text, the symmetries of the BdG Hamiltonian are not  $I$  and  $C_4$  and differ by a phase operator  $\exp(i\Phi\hat{F})$ . Here,  $\hat{F}$  is the fermion particle number operator.

This phase operator transforms  $\Delta$  as

$$\Delta(\mathbf{k}) \rightarrow \Delta(\mathbf{k}) \exp(i2\Phi). \quad (\text{A5})$$

Note that this phase operator does not influence hopping terms. When pairing terms are not invariant under  $I$  and  $C_4$ , we redefine  $I' = I \exp(i\Phi\hat{F})$  and  $C_4' = C_4 \exp(i\Phi\hat{F})$  so that  $I'$  and  $C_4'$  are explicit symmetries of pairing terms. Then inversion symmetry  $I'$  and rotational symmetry  $C_4'$  are still preserved for the system. Different choices of terms lead to different symmetries fractionalizations characterized by  $I'^2$ ,  $C_4'^4$ , and  $I'C_4'I'^{-1}C_4'^{-1}$ . We calculate these numbers for each pairing term and list them in Table IV.

The BdG Hamiltonian in the Nambu basis  $\psi_{\mathbf{k}} = (c_{\mathbf{k},\uparrow}, c_{\mathbf{k},\downarrow}, c_{-\mathbf{k},\uparrow}^\dagger, c_{-\mathbf{k},\downarrow}^\dagger)^T$  is written as

$$\hat{H}_{\text{BdG}} = \frac{1}{2} \sum_{\mathbf{k}} \psi_{\mathbf{k}}^\dagger H_{\mathbf{k}} \psi_{\mathbf{k}}, \quad (\text{A6})$$

where

$$H_{\mathbf{k}} = \begin{bmatrix} h_0(\mathbf{k}) & \Delta(\mathbf{k}) \\ \Delta^\dagger(\mathbf{k}) & -h_0^T(-\mathbf{k}) \end{bmatrix}. \quad (\text{A7})$$

We have suppressed the orbital index  $a$  in the fermion operator  $c_{\mathbf{k},a,\uparrow/\downarrow}$ . In other words, we use  $c_{\mathbf{k},\uparrow}$  to denote a spinor  $c_{\mathbf{k},\uparrow} = (c_{\mathbf{k},1,\uparrow}, \dots, c_{\mathbf{k},N,\uparrow})$ , where  $N$  is the number of bands in the system.

Due to the particle-hole symmetry, the eigenvectors  $u_{\mathbf{k},a}$  above the BdG Hamiltonian matrix  $H_{\mathbf{k}}$  at momenta  $\pm\mathbf{k}$  are related by

$$u_{-\mathbf{k},a} = \tau_x u_{\mathbf{k},a}^*, \quad (\text{A8})$$

$$H_{\mathbf{k}} u_{\mathbf{k},a} = E_a(\mathbf{k}) u_{\mathbf{k},a}, \quad H_{-\mathbf{k}} u_{-\mathbf{k},a} = -E_a(\mathbf{k}) u_{-\mathbf{k},a}, \quad (\text{A9})$$

where  $(\tau_x, \tau_y, \tau_z)$  are Pauli matrices for the Nambu index. Therefore, the eigenvectors of the BdG Hamiltonian  $H_{\mathbf{k}}$  include both ‘‘quasiparticles’’  $u_{\mathbf{k},a}$  with eigenvalue  $E_a(\mathbf{k}) \geq 0$  and ‘‘quasiholes’’  $\tau_x u_{-\mathbf{k},b}^*$  with eigenvalue  $-E_b(-\mathbf{k}) \leq 0$ . Their associated eigenmode operators are

$$\gamma_{\mathbf{k},a}^\dagger = \sum_{\alpha} u_{\mathbf{k},a,\alpha} \psi_{\mathbf{k},\alpha}^\dagger, \quad \gamma_{-\mathbf{k},b} = \sum_{\alpha} u_{-\mathbf{k},b,\alpha}^* \psi_{-\mathbf{k},\alpha}, \quad (\text{A10})$$

and the BdG Hamiltonian is diagonalized in the following form:

$$\hat{H}_{\text{BdG}} = \frac{1}{2} \sum_{\mathbf{k},a} [E_a(\mathbf{k}) \gamma_{\mathbf{k},a}^\dagger \gamma_{\mathbf{k},a} - E_a(-\mathbf{k}) \gamma_{-\mathbf{k},a} \gamma_{-\mathbf{k},a}^\dagger]. \quad (\text{A11})$$

Next, to study the optical spectrum of this model, we need to first obtain the electric current operator. The particle current operator can be calculated as a derivative of the hopping part of the Hamiltonian,

$$\hat{\mathbf{j}} = \sum_{\mathbf{k}} (c_{\mathbf{k},\uparrow}^\dagger, c_{\mathbf{k},\downarrow}^\dagger) \mathbf{j}(\mathbf{k}) (c_{\mathbf{k},\uparrow}, c_{\mathbf{k},\downarrow})^T, \quad (\text{A12})$$

with

$$\mathbf{j}(\mathbf{k}) = \frac{\partial h_0(\mathbf{k})}{\partial \mathbf{k}}. \quad (\text{A13})$$

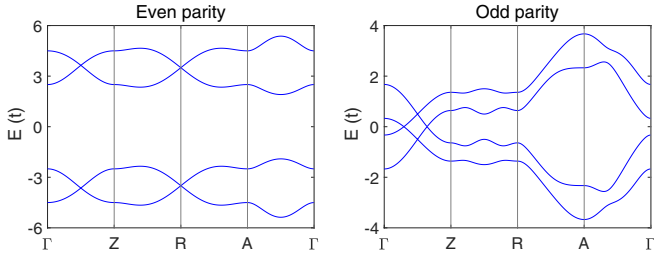


FIG. 5. Energy band of electrons. Special points in the Brillouin zone are  $\Gamma : (0, 0, 0)$ ,  $Z : (0, 0, \pi)$ ,  $R : (0, \pi, \pi)$ , and  $A : (\pi, \pi, \pi)$ . The gapless point between  $\Gamma$  and  $Z$  is part of a sphere of gapless points. For the odd-parity case, the energy gap of the first band is  $\Delta = 0.5t$ , and the energy gap of the second band is  $\Delta' = 3.5t$ . For the even-parity case, the energy gap of the first band is zero, and the energy gap of the second band is  $\Delta' = 0.5t$ .

Writing the current operator in the BdG basis  $\psi_{\mathbf{k}} = (c_{\mathbf{k},\uparrow}, c_{\mathbf{k},\downarrow}, c_{-\mathbf{k},\uparrow}^\dagger, c_{-\mathbf{k},\downarrow}^\dagger)^T$ , we have

$$\mathbf{J}(\mathbf{k}) = \begin{bmatrix} \frac{\partial h_0}{\partial \mathbf{k}}(\mathbf{k}) & 0 \\ 0 & -\frac{\partial h_0^\dagger}{\partial \mathbf{k}}(-\mathbf{k}) \end{bmatrix}, \quad (\text{A14})$$

and the current operator is

$$\hat{\mathbf{j}} = \frac{1}{2} \sum_{\mathbf{k}} \psi_{\mathbf{k}}^\dagger \mathbf{J}(\mathbf{k}) \psi_{\mathbf{k}}. \quad (\text{A15})$$

The electric current is odd under inversion. Current in the  $z$  direction  $\hat{j}_z$  is invariant under  $C_4'$ , and  $\hat{j}_x + i\hat{j}_y$  and  $\hat{j}_x - i\hat{j}_y$  are two irreducible representations that carry phase  $-i$  and  $i$  under  $C_4'$  rotation. Specifically,

$$\begin{aligned} I'(\hat{j}_x + i\hat{j}_y)I'^{-1} &= -(\hat{j}_x + i\hat{j}_y), \\ I'(\hat{j}_x - i\hat{j}_y)I'^{-1} &= -(\hat{j}_x - i\hat{j}_y), \\ I'\hat{j}_z I'^{-1} &= \hat{j}_z, \\ C_4'(\hat{j}_x + i\hat{j}_y)C_4'^{-1} &= -i(\hat{j}_x + i\hat{j}_y), \\ C_4'(\hat{j}_x - i\hat{j}_y)C_4'^{-1} &= i(\hat{j}_x - i\hat{j}_y), \\ C_4'\hat{j}_z C_4'^{-1} &= -\hat{j}_z. \end{aligned} \quad (\text{A16})$$

We calculate the current operator from (A12) as follows:

$$\begin{aligned} j_x(\mathbf{k}) &= t \cos k_x \sigma^x + m \sin k_x \sigma^z, \\ j_y(\mathbf{k}) &= t \cos k_y \sigma^y + m \sin k_y \sigma^z, \\ j_z(\mathbf{k}) &= -t_z \sin k_z \sigma^z. \end{aligned} \quad (\text{A17})$$

We show two examples.

*Case 1.*  $I'^2 = 1$ , and  $C_4'^4 = -1$ . In this case  $I' = I$  and  $C_4' = C_4$  are not changed. There is only one pairing term invariant

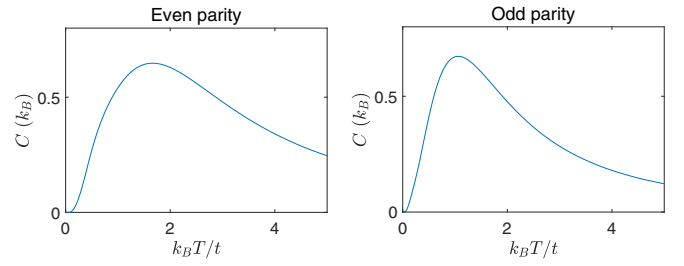


FIG. 6. Specific heat versus temperature  $T$ . The even-parity case is gapped with  $\Delta = 0.5t$ , and the specific heat is the exponential function of  $1/T$  at low temperature. The odd-parity case has gapless momentum points, and the specific heat is proportional to  $T^3$  at low temperature.

according to Table IV:

$$\Delta(\mathbf{k}) = \Delta_1 \sin k_z \sigma^x. \quad (\text{A18})$$

Here,  $\Delta_1$  is a complex number. Parameters are set as  $Q = \pi/2$ ,  $\mu = 3.5t$ ,  $m = 0.5t$ ,  $t_z = t$ , and  $\Delta_1 = t$ .

*Case 2.*  $I'^2 = -1$ ,  $C_4'^4 = -1$ ,  $I' = I \exp(i\pi \hat{F}/2)$ , and  $C_4' = C_4$ . In this case, all pairing terms with phases  $-1$  and  $1$  under the transformation of  $I'$  and  $C_4'$  are invariant under  $I'$  and  $C_4'$ . According to Table IV, pairing terms in the Hamiltonian are

$$\begin{aligned} \Delta(\mathbf{k}) &= \Delta'_1 \cos k_z i\sigma^y + \Delta'_2 (\cos k_x + \cos k_y) i\sigma^y \\ &\quad + \Delta'_3 (\sin k_x + i \sin k_y) (\sigma^0 - \sigma^z) \\ &\quad + \Delta'_4 (\sin k_x - i \sin k_y) (\sigma^0 + \sigma^z). \end{aligned} \quad (\text{A19})$$

Parameters are set as  $Q = \pi/2$ ,  $\mu = 0.3t$ ,  $m = t$ ,  $t_z = t$ , and  $\Delta'_i = 0.2t$ .

We show gapless electron bands in Fig. 5 and the specific heat in Fig. 6. The specific heat is calculated by

$$C = \frac{1}{V} \sum_i \frac{\epsilon_i^2 \exp(\epsilon_i/T)}{T^2 [1 + \exp(\epsilon_i/T)]^2}, \quad (\text{A20})$$

where  $\epsilon_i$  sums over all positive eigenvalues of the BdG Hamiltonian and index  $i$  includes the momentum index  $\mathbf{k}$  and band index  $a$ .  $V$  is the number of unit cells. The even-parity case is gapped, and the heat capacity is close to the exponential function  $\exp(-\Delta/T)$  at low temperature. The odd-parity case has gapless points, and heat capacity scales as  $T^3$  at low temperature.

We can calculate the absorption spectrum exactly using Eq. (13). For the mean-field Hamiltonian,  $|f\rangle$  can be only two-particle states. At zero temperature, the optical absorption rate is calculated by the following equations:

$$\begin{aligned} \omega \text{Im}\chi(T=0, \omega) &= \frac{\pi e^2}{2\hbar\omega} \sum_f |\langle 0 | \mathbf{e} \cdot \hat{\mathbf{j}} | f \rangle|^2 \delta(\omega - E_f + E_0) \\ &= \frac{\pi e^2}{2\hbar\omega} \sum_{\mathbf{k}, a, b} |\langle 0 | \mathbf{e} \cdot \hat{\mathbf{j}} \gamma_{\mathbf{k}, a}^\dagger \gamma_{-\mathbf{k}, b}^\dagger | 0 \rangle|^2 \delta[\omega - E_a(\mathbf{k}) - E_b(-\mathbf{k})] \end{aligned}$$

$$\begin{aligned}
&= \frac{\pi e^2}{2\hbar\omega} \sum_{\mathbf{k}, a, b, \alpha, \beta} |\mathbf{e} \cdot \mathbf{J}^{\alpha, \beta}(\mathbf{k}) \langle 0 | \psi_{\mathbf{k}, \alpha}^\dagger \psi_{\mathbf{k}, \beta} \gamma_{\mathbf{k}, a}^\dagger \gamma_{-\mathbf{k}, b}^\dagger | 0 \rangle|^2 \delta[\omega - E_a(\mathbf{k}) - E_b(-\mathbf{k})] \\
&= \frac{\pi e^2}{2\hbar\omega} \sum_{\mathbf{k}, a, b, \alpha, \beta} |\mathbf{e} \cdot \mathbf{J}^{\alpha, \beta}(\mathbf{k}) \langle 0 | \psi_{\mathbf{k}, \alpha}^\dagger \gamma_{-\mathbf{k}, b}^\dagger | 0 \rangle \langle 0 | \psi_{\mathbf{k}, \beta} \gamma_{\mathbf{k}, a}^\dagger | 0 \rangle|^2 \delta[\omega - E_a(\mathbf{k}) - E_b(-\mathbf{k})]. \quad (\text{A21})
\end{aligned}$$

Here, we apply the general formula in the first line to the BdG system. Since our current operators are only up to quadratic order of fermion operators, we excite only two quasiparticles at the same time. So the final state is specified as  $|\gamma_{\mathbf{k}, a}^\dagger \gamma_{-\mathbf{k}, b}^\dagger | 0 \rangle$  in the second line.  $a$  and  $b$  are the labels for bands of positive energy, and  $\alpha$  and  $\beta$  are the labels for the basis of the BdG Hamiltonian. In the last line, we use Wick's theorem, and this is the only contraction consistent with quantum number momentum. Since we have obtained the eigenstates of the Hamiltonian by diagonalization as

$$\gamma_{\mathbf{k}, a}^\dagger = \sum_{\alpha} u_{\mathbf{k}, a, \alpha} \psi_{\mathbf{k}, \alpha}^\dagger, \quad (\text{A22})$$

where  $u_{\mathbf{k}, a, \alpha}$  is the  $a$ th eigenvector of the BdG Hamiltonian (A7) at momentum  $\mathbf{k}$ , we can express the absorption rate more explicitly,

$$\begin{aligned}
\omega \chi''(T=0, \omega) &= \frac{\pi e^2}{2\hbar\omega} \sum_{a, b, \alpha, \beta} |u_{\mathbf{k}, b, \alpha} \mathbf{e} \cdot \mathbf{J}^{\alpha, \beta}(\mathbf{k}) u_{\mathbf{k}, a, \beta}^*|^2 \\
&\quad \times \delta[\omega - E_a(\mathbf{k}) - E_b(-\mathbf{k})]. \quad (\text{A23})
\end{aligned}$$

Here, index  $a$  is summed over bands of positive energy  $E_a(\mathbf{k})$ , and index  $b$  is summed over bands of negative energy  $E_b(\mathbf{k})$ .

In Fig. 7, we show the absorption spectrum of our model under a polarized beam of light. The left and right columns represent two models, and they reveal stark contrasts in the spectrum. The spectrum on the left ( $I^2 = 1$ ) is normal, with

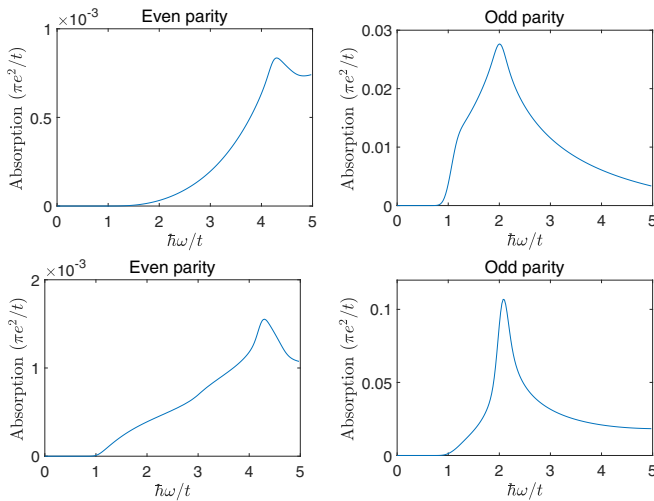


FIG. 7. Absorption spectra are intensity  $I$  versus photon energy  $\hbar\omega$ . The spectrum corresponds to models with  $I^2 = 1$  and polarization in the  $z$  direction (top left) and  $x$  direction (bottom left). In comparison, we show the spectrum of the model with  $I^2 = -1$  and polarization in the  $z$  direction (top right) and  $x$  direction (bottom right).

nonzero amplitude above energy gap  $2\Delta \approx t$ . In contrast, the spectrum on the right ( $I^2 = -1$ ) is a flat line of zero at low energy above energy gap  $2\Delta = 0$  that becomes finite only above the energy threshold  $\Delta + \Delta' \approx 0.5t$ , indicating the selection rule of  $I^2 = -1$ . One detail is that the spectrum is not zero even when  $\omega$  is a little bit higher than  $0.5t$ . That is because the band bottoms of the first and second bands do not occur at the same momentum. This difference underscores the importance of inversion symmetry fractionalization on the absorption spectrum of superconductors.

We show Raman spectra of both models in Fig. 8. We calculate the Raman differential scattering cross section per volume from Eq. (20):

$$\frac{1}{V} \frac{\partial^2 \sigma}{\partial \Omega \partial \omega_s} = \frac{e^4}{\hbar V} \frac{\omega_s}{\omega_i} \sum_f |\langle f | e_i^\alpha e_s^\beta M^{\alpha\beta} | i \rangle|^2 \delta(\omega + E_i - E_f),$$

where  $V$  is the number of unit cells. This calculation is more complex but can still be done accurately for mean-field theory. We make use of Eq. (21) and calculate the expectation value for excitation of two-particle states. This calculation is done using Wick's theorem in a manner similar to the calculation of the absorption spectrum. It is worth mentioning that four-particle states  $|f\rangle$  have zero scattering amplitude  $M$  and do not contribute to Raman scattering in the mean-field calculation. For further details about this calculation, refer to Refs. [24,32,33].

The Raman spectrum has the selection rule for the even-parity case, which is opposite the selection rule of the absorption spectrum. In the even-parity case, Raman scattering is zero below  $\Delta + \Delta' \approx 4t$  because of the selection rule. In the odd-parity case, Raman scattering is not zero at any frequency because the band is gapless.

## APPENDIX B: SINGLET SUPERCONDUCTIVITY IN DOPED GRAPHENE

Our second example is a 2D system on a honeycomb lattice without spin-orbital coupling, where  $SU(2)$  spin

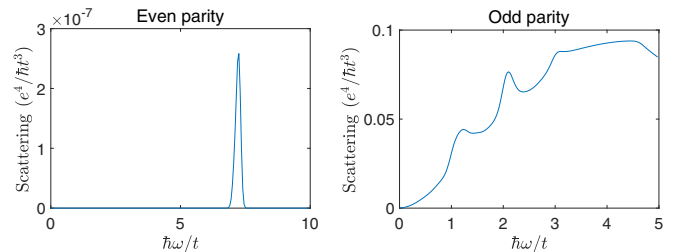


FIG. 8. Differential scattering cross sections of both incident and scattered light polarized in the  $x$  direction, corresponding to  $I^2 = 1$  (left) and  $I^2 = -1$  (right).



rotational symmetry, space inversion symmetry, and  $C_3$  rotational symmetry are all preserved. With a beam of light, only a spin-singlet pair of excitations at  $\mathbf{k}$  and  $-\mathbf{k}$  is excited. Inversion symmetry can also have selection rules in this case. Whether the spectrum is zero or not depends on whether inversion is  $I^2 = 1$  or  $-1$ .

To be specific, if  $I^2 = 1$ , we can choose a gauge such that under inversion  $I'$ ,

$$\begin{aligned} I' \gamma_{\mathbf{k},\uparrow} I'^{-1} &= \gamma_{-\mathbf{k},\uparrow}, \\ I' \gamma_{\mathbf{k},\downarrow} I'^{-1} &= \gamma_{-\mathbf{k},\downarrow}. \end{aligned} \quad (\text{B1})$$

This leads to the action of inversion on the excitation of the singlet pair,

$$\begin{aligned} I' (\gamma_{\mathbf{k},\uparrow} \gamma_{-\mathbf{k},\downarrow} - \gamma_{\mathbf{k},\downarrow} \gamma_{-\mathbf{k},\uparrow}) I'^{-1} \\ = \gamma_{-\mathbf{k},\uparrow} \gamma_{\mathbf{k},\downarrow} - \gamma_{-\mathbf{k},\downarrow} \gamma_{\mathbf{k},\uparrow} = \gamma_{\mathbf{k},\uparrow} \gamma_{-\mathbf{k},\downarrow} - \gamma_{\mathbf{k},\downarrow} \gamma_{-\mathbf{k},\uparrow}. \end{aligned} \quad (\text{B2})$$

Therefore, this excitation is even under inversion, and there will be no absorption spectrum because current is odd,  $I' \hat{j} I'^{-1} = -\hat{j}$ .

On the other hand, if  $I^2 = -1$ , under a certain gauge, the action of inversion on fermions is

$$\begin{aligned} I' \gamma_{\mathbf{k},\uparrow} I'^{-1} &= \gamma_{-\mathbf{k},\uparrow}, \\ I' \gamma_{\mathbf{k},\downarrow} I'^{-1} &= -\gamma_{-\mathbf{k},\downarrow}, \end{aligned} \quad (\text{B3})$$

and we have one extra minus sign, and excitation is odd under inversion. In this case, optical absorption is allowed.

With this general rule in mind, we write down a tight-binding model on the honeycomb lattice explicitly. The total Hamiltonian will still be in the form of Eqs. (A7) and (A6). The only difference is operator  $\Psi_k = (c_{1,\mathbf{k},\uparrow}, c_{2,\mathbf{k},\uparrow}, c_{1,-\mathbf{k},\downarrow}^\dagger, c_{2,-\mathbf{k},\downarrow}^\dagger)^T$ . Here, labels 1 and 2 indicate the sublattice number.

We consider only on-site and nearest-neighbor terms. Due to the  $SU(2)$  spin rotational symmetry, hopping terms between two sites can be only  $t \hat{c}_{i,\uparrow}^\dagger \hat{c}_{j,\uparrow} + t \hat{c}_{i,\downarrow}^\dagger \hat{c}_{j,\downarrow} + \text{H.c.}$  It is even under link center inversion when  $t$  is real and odd when  $t$  is imaginary. The pairing term can be only  $\Delta \hat{c}_{i,\uparrow} \hat{c}_{j,\downarrow} - \Delta \hat{c}_{i,\downarrow} \hat{c}_{j,\uparrow} + \text{H.c.}$  and is even under permutations of  $i$  and  $j$ .

The hopping term of the Hamiltonian is invariant under inversion and  $C_3$  rotational symmetry:

$$\begin{aligned} I : \quad h_0(-\mathbf{k}) &= \sigma^x h_0(\mathbf{k}) \sigma^x, \\ C_3 : \quad h_0(-k_2, k_1 - k_2) &= S^\dagger h_0(k_1, k_2) S, \end{aligned} \quad (\text{B4})$$

where  $(k_1, k_2)$  are the coordinates of the two reciprocal lattice vectors, meaning  $\mathbf{k} = k_1 \hat{k}_1 + k_2 \hat{k}_2$ , and  $S$  is the matrix

$$S = \begin{bmatrix} 1 & \\ & e^{-ik_2} \end{bmatrix}. \quad (\text{B5})$$

Symmetry-allowed hopping terms are the chemical potential and  $C_3$ -invariant real hopping between nearest neighbors. The general form of the hopping term of the Hamiltonian in momentum space is

$$h_0(\mathbf{k}) = \begin{bmatrix} \mu & t(1 + e^{ik_1} + e^{ik_2}) \\ t(1 + e^{-ik_1} + e^{-ik_2}) & \mu \end{bmatrix}. \quad (\text{B6})$$

Here,  $t$  and  $\mu$  are real numbers.

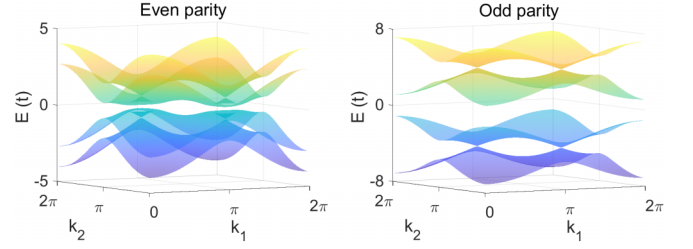


FIG. 9. Electron bands for two cases. The even-parity case has a small gap. The energy gap of the first band is  $\Delta = 0.22t$ , and the second band gap is  $\Delta' = 0.75t$ . The odd-parity case is gapless, with the first band gap  $\Delta = 1.1t$  and the second band gap  $\Delta' = 4.2t$ .

Next, the current operator  $j^z$  is zero, and  $j^{x,y}$  have the following form:

$$\begin{aligned} j_x(\mathbf{k}) &= \begin{bmatrix} i \frac{t}{2} (e^{ik_1} - e^{ik_2}) \\ -i \frac{t}{2} (e^{-ik_1} - e^{-ik_2}) \end{bmatrix}, \\ j_y(\mathbf{k}) &= \begin{bmatrix} i \frac{\sqrt{3}t}{6} (-2 + e^{ik_1} + e^{ik_2}) \\ -i \frac{\sqrt{3}t}{6} (-2 + e^{-ik_1} + e^{-ik_2}) \end{bmatrix}. \end{aligned} \quad (\text{B7})$$

To write down the pairing term of the Hamiltonian explicitly, we need to fix inversion symmetry fractionalization. Below we consider two different kinds of pairing with  $I^2 = \pm 1$ .

*Case 1.* Inversion symmetry is  $I' = I$ , i.e.,  $I^2 = 1$ . Pairing terms are invariant under symmetry  $I'$ , and  $C_3$  are on-site and nearest-neighbor pairings of the same strength. The pairing terms in the Hamiltonian are

$$\Delta(\mathbf{k}) = \begin{bmatrix} \Delta & \Delta_1(1 + e^{ik_1} + e^{ik_2}) \\ \Delta_1^*(1 + e^{-ik_1} + e^{-ik_2}) & \Delta \end{bmatrix}. \quad (\text{B8})$$

The parameters are  $\mu = 0.5t$  and  $\Delta = \Delta_1 = 0.5t$ .

*Case 2.* Inversion symmetry is  $I' = I \exp(i\pi \hat{F}/2)$ , i.e.,  $I^2 = -1$ . The pairing term in the Hamiltonian is

$$\Delta(\mathbf{k}) = \Delta_2 \sigma^z. \quad (\text{B9})$$

The parameters are  $\mu = t$  and  $\Delta_2 = 4t$ .

Now we calculate the observable quantities for this mode. The calculation is the same as that for the case without  $SU(2)$  symmetry.

We show electron bands for two cases in Fig. 9 and the specific heat in Fig. 10. Both cases are gapped, and specific heat is  $C \approx \exp(\Delta/T)$  at low temperature.

The absorption spectrum can be calculated based on Eq. (A21). We use light polarized in the  $x$  direction. The absorption spectrum of these two cases is shown in Fig. 11. On the left is the model with  $I^2 = 1$ , and on the right is the model with  $I^2 = -1$ . It is clear that the spectrum satisfies the selection rule for the even-parity case. For the even-parity case, the spectrum is zero from energy gap  $2\Delta = 0.44t$  to  $\Delta + \Delta' = 0.97t$ . For the odd-parity case, the spectrum is not zero above energy gap  $2\Delta = 2.2t$ .

The Raman spectrum is shown in Fig. 12. The odd-parity case shows the selection rule. For the even-parity case, scattering is not zero above energy gap  $2\Delta$ . But for the odd-parity case, scattering is zero between energy gaps  $2\Delta$  and  $\Delta + \Delta'$ .

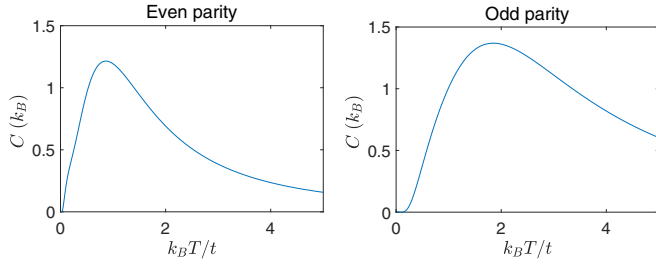


FIG. 10. Specific heat versus temperature  $T$ . Both the even-parity and odd-parity cases are gapped, and specific heat is an exponential function of  $1/T$  at low temperature. The energy gap is  $\Delta = 0.22t$  for the even-parity case and  $\Delta = 0.56t$  for the odd-parity case.

### APPENDIX C: DISCUSSION OF SELECTION RULES FOR GENERAL POINT GROUP SYMMETRIES

In this Appendix we systematically study possible selection rules in the case of a general point group. Our discussion includes the case of a unitary point group  $G_{\text{total}} = G$  and the case of a magnetic point group that can be written as  $G_{\text{total}} = G + AG$ , where  $G$  is the unitary subgroup and  $AG$  is the coset corresponding to an antiunitary symmetry  $A$  (including but not restricted to time reversal symmetry).

In the same spirit as the case of inversion symmetry, we want to ask whether the strength of the spectrum contributed by pair excitation from the lowest bands is constrained to vanish by symmetry. Specifically, we want to study, for general momentum  $\mathbf{k}$ , whether the matrix element

$$\langle 0 | \hat{O} \gamma_{\mathbf{k},0}^\dagger \gamma_{-\mathbf{k},0}^\dagger | 0 \rangle \quad (\text{C1})$$

is zero. Here,  $\hat{O}$  represents the current operator  $\hat{j}$  for the absorption spectrum and the Raman operator  $R$  for the Raman spectrum. To study the effect of symmetry on this, we study the representation of pair excitation states

$$|f_{\mathbf{k}}\rangle = \gamma_{\mathbf{k},0}^\dagger \gamma_{-\mathbf{k},0}^\dagger | 0 \rangle. \quad (\text{C2})$$

We decompose the representation  $\{|f_{g(\mathbf{k})}\rangle, g \in G_{\text{total}}\}$  into irreducible representations and check whether it can form a trivial representation after combining with operator  $\hat{O}$ . If it cannot, the matrix element transforms nontrivially under the symmetry group and is constrained to be zero; hence, we have the selection rule. Otherwise, the spectrum does not vanish. In the special case of  $\{|f_{\mathbf{k}}\rangle\}$  having all the representations of

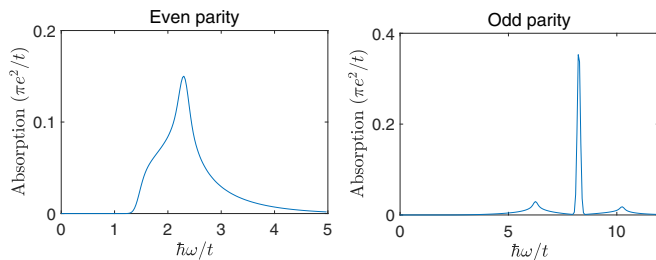


FIG. 11. Absorption spectrum of models with  $I^2 = 1$  and polarization in the  $x$  direction (left). In comparison, we show the spectrum of the model with  $I^2 = -1$  and polarization in the  $x$  direction (right).

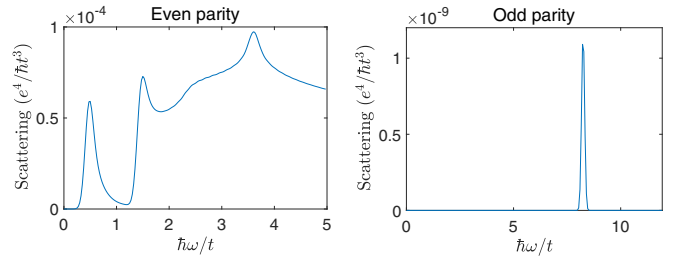


FIG. 12. Differential scattering cross section of both incident and scattered light polarized in the  $x$  direction, corresponding to  $I^2 = 1$  (left) and  $I^2 = -1$  (right).

group  $G_{\text{total}}$ , there is no selection rule since the result does not depend on representations of operator  $\hat{O}$ .

Let us consider a general momentum  $\mathbf{k}$ . The only symmetries that do not change the  $\mathbf{k}$ ,  $-\mathbf{k}$  pair are inversion symmetry  $I$ , time reversal symmetry  $T$ , and their product  $TI$ . In the following, we divide the problem into several cases and discuss them in detail.

*Case 1.* For unitary point group  $G$  with inversion  $I \notin G$ ,  $\{|f_{\mathbf{k}}\rangle\}$  forms unitary representations of group  $G$ . Since inversion is not in  $G$ , all  $g(\mathbf{k})$  are different, and  $\{|f_{\mathbf{k}}\rangle\}$  forms the  $|G|$ -dimensional fundamental representation of  $G$ . Since fundamental representation contains all irreducible representations, there is no selection rule in this case.

*Case 2.* For unitary point group  $G$  with inversion  $I \in G$ , every group element other than  $I$  will change momentum. So  $\{|f_{\mathbf{k}}\rangle\}$  forms fundamental representation of  $G/Z_2^I$  ( $Z_2^I$  is the  $Z_2$  group of inversion). As the representation of  $G$ , depending on  $I = +1$  or  $I = -1$ ,  $\{|f_{\mathbf{k}}\rangle\}$  contains half of the irreducible representations and is missing the other half. This gives us the selection rule of inversion symmetry, as discussed before. There are no other selection rules.

Below we discuss the case of magnetic point groups with antiunitary symmetries, where  $\{|f_{\mathbf{k}}\rangle\}$  forms the corepresentation of the symmetry group [43]. One property we will use is that the corepresentations of  $G + AG$  have a one-to-one correspondence with the representations of the unitary subgroup  $G$ . To see which corepresentation is present, we can simply forget about the antiunitary part and determine which representation of  $G$  is present.

*Case 3.* For magnetic point group  $G_{\text{total}} = G + AG$  with inversion  $I \notin G$ ,  $\{|f_{\mathbf{k}}\rangle\}$  forms the fundamental representation of  $G$  as in case 1. Therefore, it contains every corepresentation of  $G_{\text{total}}$ , and there is no selection rule.

*Case 4.* For magnetic point group  $G_{\text{total}} = G + AG$  with inversion  $I \in G$  and time reversal  $T \notin AG$ , following the same logic, this case is the same as case 2.  $\{|f_{\mathbf{k}}\rangle\}$  contains half of the irreducible corepresentations of  $G_{\text{total}}$  depending on  $I = +1$  or  $I = -1$ . This gives us the selection rule of inversion symmetry.

*Case 5.* Magnetic point group  $G_{\text{total}} = G + AG$  with inversion  $I \in G$  and time reversal  $T \in AG$  is a special case because  $IT$  guarantees a twofold band degeneracy. We have states

$$|f_{\mathbf{k},\alpha,\beta}\rangle = \gamma_{\mathbf{k},0,\alpha}^\dagger \gamma_{-\mathbf{k},0,\beta}^\dagger | 0 \rangle, \quad (\text{C3})$$

where  $\alpha, \beta = 1, 2$  are the labels of the degenerate bands. We pick up states with  $\alpha = 1$  and  $\beta = 2$  and realize

$|f_{\mathbf{k},1,2}\rangle$  and  $|f_{-\mathbf{k},1,2}\rangle$  are two different states. So  $\{|f_{\mathbf{k},1,2}\rangle\}$  forms a fundamental representation of  $G$ . Since  $\{|f_{\mathbf{k},1,2}\rangle\}$  already has all irreducible representations, the matrix element (C1) is nonzero, and there is no selection rule in this case.

In conclusion, selection rules arise only for inversion symmetry (and  $C_{2,z}$  symmetry in two dimensions, which acts like inversion symmetry). No other crystal symmetries or magnetic crystal symmetries lead to nontrivial selection rules in optical and Raman spectroscopy.

- 
- [1] C. L. Degen, F. Reinhard, and P. Cappellaro, *Rev. Mod. Phys.* **89**, 035002 (2017).
- [2] M. Kjaergaard, M. E. Schwartz, J. Braumüller, P. Krantz, J. I.-J. Wang, S. Gustavsson, and W. D. Oliver, *Annu. Rev. Condens. Matter Phys.* **11**, 369 (2020).
- [3] J. L. MacManus-Driscoll and S. C. Wimbush, *Nat. Rev. Mater.* **6**, 587 (2021).
- [4] J. F. Annett, *Adv. Phys.* **39**, 83 (1990).
- [5] M. Sigrist and K. Ueda, *Rev. Mod. Phys.* **63**, 239 (1991).
- [6] C. C. Tsuei and J. R. Kirtley, *Rev. Mod. Phys.* **72**, 969 (2000).
- [7] A. Damascelli, Z. Hussain, and Z.-X. Shen, *Rev. Mod. Phys.* **75**, 473 (2003).
- [8] P. A. Lee, N. Nagaosa, and X.-G. Wen, *Rev. Mod. Phys.* **78**, 17 (2006).
- [9] L. Taillefer, *Annu. Rev. Condens. Matter Phys.* **1**, 51 (2010).
- [10] N. P. Armitage, P. Fournier, and R. L. Greene, *Rev. Mod. Phys.* **82**, 2421 (2010).
- [11] Y. Ando and L. Fu, *Annu. Rev. Condens. Matter Phys.* **6**, 361 (2015).
- [12] M. Sato and Y. Ando, *Rep. Prog. Phys.* **80**, 076501 (2017).
- [13] C. Nayak, S. H. Simon, A. Stern, M. Freedman, and S. Das Sarma, *Rev. Mod. Phys.* **80**, 1083 (2008).
- [14] J. Alicea, *Rep. Prog. Phys.* **75**, 076501 (2012).
- [15] C. Beenakker, *Annu. Rev. Condens. Matter Phys.* **4**, 113 (2013).
- [16] R. M. Lutchyn, E. P. A. M. Bakkers, L. P. Kouwenhoven, P. Krogstrup, C. M. Marcus, and Y. Oreg, *Nat. Rev. Mater.* **3**, 52 (2018).
- [17] D. J. Van Harlingen, *Rev. Mod. Phys.* **67**, 515 (1995).
- [18] D. J. Scalapino, *Phys. Rep.* **250**, 329 (1995).
- [19] N. Read and D. Green, *Phys. Rev. B* **61**, 10267 (2000).
- [20] X. Yang, S. Lu, S. Biswas, M. Randeria, and Y.-M. Lu, [arXiv:2401.00321](https://arxiv.org/abs/2401.00321).
- [21] Y. Cao, V. Fatemi, S. Fang, K. Watanabe, T. Taniguchi, E. Kaxiras, and P. Jarillo-Herrero, *Nature (London)* **556**, 43 (2018).
- [22] K. Shiozaki, *Prog. Theor. Exp. Phys.* **2022**, 04A104 (2022).
- [23] J. Ahn and N. Nagaosa, *Nat. Commun.* **12**, 1617 (2021).
- [24] T. P. Devereaux and R. Hackl, *Rev. Mod. Phys.* **79**, 175 (2007).
- [25] L. Schwarz *et al.*, *Nat. Commun.* **11**, 287 (2020).
- [26] R. Shimano and N. Tsuji, *Annu. Rev. Condens. Matter Phys.* **11**, 103 (2020).
- [27] G. D. Mahan, *Superconductivity* (Springer, Boston, MA, 2000), pp. 627–675.
- [28] K.-Y. Yang, Y.-M. Lu, and Y. Ran, *Phys. Rev. B* **84**, 075129 (2011).
- [29] G. Y. Cho, J. H. Bardarson, Y.-M. Lu, and J. E. Moore, *Phys. Rev. B* **86**, 214514 (2012).
- [30] Y. Li and F. D. M. Haldane, *Phys. Rev. Lett.* **120**, 067003 (2018).
- [31] A. Altland and M. R. Zirnbauer, *Phys. Rev. B* **55**, 1142 (1997).
- [32] B. S. Shastry and B. I. Shraiman, *Phys. Rev. Lett.* **65**, 1068 (1990).
- [33] B. S. Shastry and B. I. Shraiman, *Int. J. Mod. Phys. B* **5**, 365 (1991).
- [34] E. Lake, A. S. Patri, and T. Senthil, *Phys. Rev. B* **106**, 104506 (2022).
- [35] G. R. Stewart, *Adv. Phys.* **66**, 75 (2017).
- [36] Y. Maeno, S. Kittaka, T. Nomura, S. Yonezawa, and K. Ishida, *J. Phys. Soc. Jpn.* **81**, 011009 (2012).
- [37] Y. Liu and Z.-Q. Mao, *Phys. C (Amsterdam, Neth.)* **514**, 339 (2015).
- [38] K. E. Avers *et al.*, *Nat. Phys.* **16**, 531 (2020).
- [39] D. Aoki, J.-P. Brison, J. Flouquet, K. Ishida, G. Knebel, Y. Tokunaga, and Y. Yanase, *J. Phys.: Condens. Matter* **34**, 243002 (2022).
- [40] D. C. Mattis and J. Bardeen, *Phys. Rev.* **111**, 412 (1958).
- [41] L. Leplae, *Phys. Rev. B* **27**, 1911 (1983).
- [42] W. Zimmermann, E. Brandt, M. Bauer, E. Seider, and L. Genzel, *Phys. C (Amsterdam, Neth.)* **183**, 99 (1991).
- [43] C. Bradley and B. Davies, *Rev. Mod. Phys.* **40**, 359 (1968).